

# Systematics-insensitive periodic signal search with K2

Ruth Angus<sup>1,3</sup> Daniel Foreman-Mackey<sup>2</sup> & John A. Johnson<sup>3</sup>

## ABSTRACT

From pulsating stars to transiting exoplanets, the search for periodic signals in *K2* data, *Kepler's* 2-wheeled extension, is relevant to a long list of scientific goals. Systematics affecting *K2* light curves due to the decreased spacecraft pointing precision inhibit the easy extraction of periodic signals from the data. We here develop a method for producing periodograms of *K2* light curves that are insensitive to pointing-induced systematics; the Systematics-Insensitive Periodogram (SIP). Traditional sine-fitting periodograms use a generative model to find the frequency of a sinusoid that best describes the data. We extend this principle by including systematic trends, based on a set of ‘Eigen light curves’, following Foreman-Mackey et al. (2015), in our generative model as well as a sum of sine and cosine functions over a grid of frequencies. Using this method we are able to produce periodograms with vastly reduced systematic features. The quality of the resulting periodograms are such that we can recover acoustic oscillations in giant stars and measure stellar rotation periods without the need for any detrending. The algorithm is also applicable to the detection of other periodic phenomena such as variable stars, eclipsing binaries and short-period exoplanet candidates. The SIP code is available at <https://github.com/RuthAngus/SIPK2>.

*Subject headings:* asteroseismology — methods: statistical — methods: data analysis — stars: rotation — techniques: photometric

## 1. Introduction

The excellent precision achieved by the original *Kepler* mission relied on extremely precise pointing, for which three reaction wheels were required. After the failure of one of these wheels, the *Kepler* team devised a new pointing scheme in which the spacecraft

---

<sup>1</sup>Subdepartment of Astrophysics, University of Oxford, OX1 3RH, UK, ruthangus@gmail.com

<sup>2</sup>Center for Cosmology and Particle Physics, New York University, NY, USA

<sup>3</sup>Harvard-Smithsonian Center for Astrophysics, 60 Garden St., Cambridge, MA, USA

is stabilized by the Solar wind for ecliptic plane viewing zones (Howell et al. 2014). In this configuration the spacecraft is able to maintain an unstable equilibrium, with the two functioning reaction wheels controlling pitch and yaw whilst the spacecraft slowly rolls about the boresight. The spacecraft fires its thrusters once every  $\sim 6$  hours (Vanderburg and Johnson 2014, hereafter VJ14) to correct for this slow drift and, as stars move across pixels with different sensitivities, their flux varies. The extraction of high-precision photometry from *K2* target pixel files, despite the reduced pointing precision, is a requirement for many fields of research and several methods for the extraction and detrending of *K2* light curves have already been developed. For example, VJ14 and Crossfield et al. (2015) use simple aperture photometry and correct the light curve of each star individually and Aigrain et al. (2015) use a Gaussian process to model the non-linear dependence of stellar flux on the roll angle of the telescope.

Whilst these methods successfully remove most systematic trends and produce light curves suitable for exoplanet search and some stellar variability studies, residual systematics can still affect the light curves on timescales relevant to asteroseismology and stellar rotation. In particular, the  $\sim 6$  hour thruster firing signal may still appear with high power in the periodograms of these detrended light curves (see figure 1). A detrending method for *K2* light curves, specifically intended for the asteroseismic analysis of giant stars has been developed by Lund et al. (2015), in which the systematics due to roll are corrected, again on a star-by-star basis and any remaining periodic signals at  $47 \mu\text{Hz}$  (6 hour period) or its harmonics are removed by prewhitening. The method developed here, the Systematics-Insensitive Periodogram (SIP) produces periodograms of *K2* light curves without the need for detrending or prewhitening.

### 1.1. Asteroseismology

As well as providing data that have led to the discovery of thousands of exoplanets, the original *Kepler* mission revolutionized many fields of stellar astronomy, particularly asteroseismology. Fundamental stellar parameters—in some cases, extremely precise ones—can be calculated for *Kepler* asteroseismic stars from the power spectra of their light curves. Although Sun-like stars oscillate at high frequencies and require short-cadence observations, pulsations of giant stars lie below the Nyquist frequency set by the 28.5 minute sampling rate of long cadence *Kepler* data:  $283 \mu\text{Hz}$ . Asteroseismic analysis of data from the original *Kepler* mission is traditionally conducted upon detrended light curves. For short cadence *Kepler* data, this detrending method is described in García et al. (2011). Due to the precise pointing of the original *Kepler* mission, systematics present in these light curves, caused by

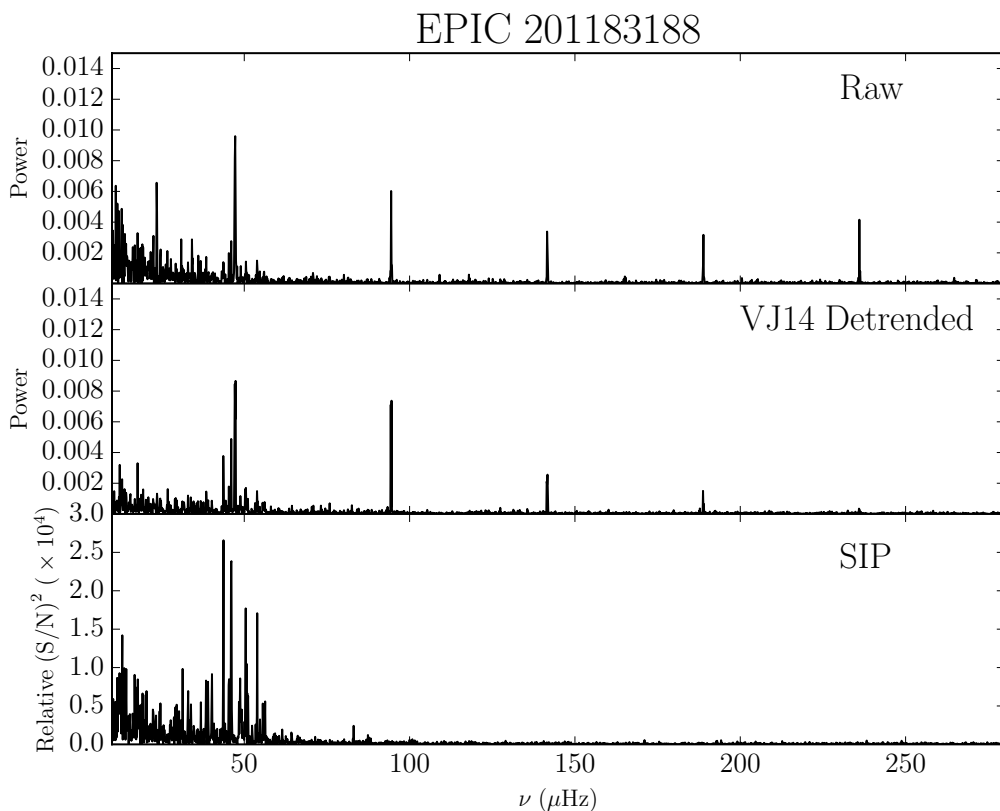


Fig. 1.— LS periodograms of the raw (Top) and VJ14–detrended (middle) *K2* light curves of EPIC 201183188. The bottom panel shows the SIP for this target. Peaks at  $\sim 47 \mu\text{Hz}$  and its harmonics produced by the regular spacecraft thruster fires are still present in the LS periodogram of the detrended data, but do not appear in the SIP.

temperature fluctuations and minor pointing shifts, are relatively low amplitude.

However, this is not the case for *K2* light curves: the precision over a 6 hour timescale is estimated to be 4 times worse in *K2* data (Howell et al. 2014), therefore new approaches to the treatment of systematics are necessary. Figure 1 demonstrates the need for careful systematics treatment of *K2* photometry for asteroseismology. The top panel shows a Lomb-Scargle<sup>1</sup> (LS) periodogram of the raw, simple aperture photometry<sup>2</sup> of EPIC 201183188, a pulsating giant star. The large peaks at  $\sim 47 \mu\text{Hz}$  and its harmonics are caused by the regular thruster fires of the spacecraft. The bottom panel shows the LS periodogram of this light curve, after it has been detrended using the method of VJ14. The large peaks are still present in the detrended light curve. While this remaining noise source does not interfere with the detection of high-signal-to-noise transit events for periods greater than  $\sim 1$  day (Vanderburg et al. 2015), it does hamper the detection of smaller signals, particularly on time scales comparable to that of thruster fires. These peaks lie in an important region of parameter space for giant star asteroseismology and could affect the stellar parameters measured for thousands of giants if not dealt with appropriately.

## 1.2. Stellar rotation

Stellar rotation studies have hugely benefitted from the era of high-precision space photometry. Active regions on the surface of rotating stars produce periodic variations in flux and stellar rotation periods can therefore be measured from *Kepler* light curves. Stellar rotation is a field of active interest as the rotation period of star can be used to infer its age via gyrochronology (Skumanich 1972; Barnes 2007; Epstein and Pinsonneault 2014; Angus et al. 2015), is thought to be tied to the stellar magnetic dynamo, and could even reveal dynamical interactions with companion stars or planets (e.g. Béky et al. 2014; Poppenhaeger and Wolk 2014). Current methods for measuring rotation periods from *Kepler* light curves include periodogram (e.g. Reinhold and Reiners 2013), AutoCorrelation Function (ACF) (McQuillan et al. 2013a) and wavelet (e.g. García et al. 2014) analysis, or some combination thereof. Stellar variability is not typically sinusoidal, therefore sine-fitting periodograms are not perfectly suited to measuring rotation periods (McQuillan et al. 2013a). For this reason, the ACF method is often favoured over the periodogram method. However, because auto-correlation is performed directly on detrended light curves, and cannot be written down as a

---

<sup>1</sup>All LS periodograms produced in this project were produced using the gatspy Python module: <https://github.com/astroML/gatspy/tree/master/gatspy/periodic>

<sup>2</sup>The method used to extract this photometry is described in §2

generative model, it is not possible use autocorrelation techniques on untreated *K2* data. A quasi-periodic Gaussian process is a much better effective model for stellar variability than a sinusoid, however we choose to focus on the more generally applicable (and computationally tractable) sine-wave periodogram, leaving the Gaussian process periodogram for future consideration.

In this article we focus on the examples of asteroseismology and stellar rotation, however many other fields of astronomy utilize periodic information in *K2* light curves. These include studies of eclipsing binaries, variable stars, exoplanets, white dwarfs and even AGN. The development of tools for extracting periodic information from *K2* data is essential if it is to be as revolutionary in time-domain astronomy as the original *Kepler* mission was.

In §2 we outline the method behind the SIP. In §3 we apply the SIP to real *K2* light curves, using some giant asteroseismic pulsators and rotating stars as test cases and then provide the results of some simple tests which show exactly *how* ‘insensitive’ the SIP is to systematic features. Finally, we demonstrate the SIP’s usefulness regarding other periodically varying objects in this section, before presenting our conclusions in §4.

## 2. Method

The method implemented in this article is an extension of the planet-search algorithm developed by Foreman-Mackey et al. (2015) (hereafter FM15). All targets observed by *Kepler* move on the CCD in the same way, therefore the systematics affecting each individual star’s light curve have shared properties. The FM15 method uses this fact by decomposing the light curves into a set of ‘Eigen Light Curves’ (ELCs) using Principle Component Analysis (PCA), which can be used to model any individual star’s light curve with very little loss of information. This process is similar to the method used to produce PDC-MAP data for the original *Kepler* mission (Stumpe et al. 2012; Smith et al. 2012). The resulting ELCs from campaign 1 can be used to model any campaign 1 *K2* light curve, (campaign 0 ELCs for campaign 0, etc) and specifically, can model the data in combination with an arbitrary physical model.

In order to construct sets of ELCs for campaigns 0 and 1, FM15 downloaded the target pixel files for all stars in these two fields. The position of each star was predicted using the World Coordinate System (WCS) and 10 circular apertures placed around the star with radii varying from 1 to 5 pixels in steps of 0.5 pixels. Following the procedure of VJ14, the aperture producing the light curve with the lowest CDPP within a 6 hour window (Christiansen et al.

2012) was selected<sup>3</sup>. PCA was then performed on the full set of targets in order to produce ELCs.

FM15 used 150 of these ELCs, plus a transit model, in order to search for exoplanet candidates without the need for a ‘detrending’ step. The likelihood of the data, conditioned on the ELC-plus-transit model was calculated over a fine grid of periods and transit depths, resulting in the detection of 36 new exoplanet candidates. We use a very similar technique to find periodic signals in K2 data. The primary difference is that we use a sinusoid rather than a transit model. This model is linear, therefore the likelihood function conditioned on a specific frequency can be calculated and the systematics model marginalized over analytically.

Following the notation in FM15, our model for the  $k$ th star can be written

$$\mathbf{f}_k = \mathbf{A}\mathbf{w}_k + \text{noise}, \quad (1)$$

where  $\mathbf{f}_k$  is the vector of  $N$  flux values,

$$\mathbf{f}_k = (f_{k,1}, f_{k,2}, f_{k,3}, \dots, f_{k,N})^T \quad (2)$$

at times

$$\mathbf{t}_k = (t_1, t_2, t_3, \dots, t_N)^T. \quad (3)$$

$\mathbf{A}$  is the design matrix:

$$\mathbf{A} = \begin{pmatrix} x_{1,1} & x_{2,1} & \cdots & x_{150,1} & 1 & \sin(2\pi\nu t_1) & \cos(2\pi\nu t_1) \\ x_{1,2} & x_{2,2} & \cdots & x_{150,2} & 1 & \sin(2\pi\nu t_2) & \cos(2\pi\nu t_2) \\ & & \vdots & & & & \\ x_{1,N} & x_{2,N} & \cdots & x_{150,N} & 1 & \sin(2\pi\nu t_N) & \cos(2\pi\nu t_N) \end{pmatrix} \quad (4)$$

where the  $x_{ij}$ s are the ELCs<sup>4</sup>, with  $i$  denoting the ELC number and  $j$  the time index. The design matrix contains the basis functions of the linear model. The basis functions for the systematic features in the light curves are the ELC values at each time index, the sine and cosine terms are the basis functions of the sinusoidal signal of interest, and the ‘1’s describe a linear offset. Any *K2* light curve can be reproduced as a linear combination of these basis functions. We are interested in the last two elements of the weight vector: the coefficients of the sinusoidal signal. The maximum likelihood solution for the weight vector,  $\mathbf{w}$  is

$$\mathbf{w}_k^* \leftarrow (\mathbf{A}^T \mathbf{A})^{-1} \mathbf{A}^T \mathbf{f}_k. \quad (5)$$

---

<sup>3</sup>The simple aperture photometry light curves for campaigns 0 and 1 are available at <http://bbq.dfm.io/ketu/lightcurves/>

<sup>4</sup>Campaign 0 and 1 ELCs are available at <http://bbq.dfm.io/ketu/elcs/>

Under this linear model with Gaussian uncertainties, the marginalized likelihood for the periodic amplitude is a two-dimensional Gaussian with mean given by the last two elements ( $\mathbf{a}$ ) of  $\mathbf{w}^*$  and covariance given by the bottom right two-by-two block ( $\mathbf{S}_a$ ) of  $(\mathbf{A}^T \mathbf{C}^{-1} \mathbf{A})^{-1}$ , where the  $\mathbf{C}$  matrix contains observational uncertainties on the diagonal. These uncertainties are estimated as  $1.48 \times$  the Median Absolute Deviation (MAD), following Aigrain et al. (2015). Therefore, the signal-to-noise ratio,  $S/N$  of the amplitude measurement is  $\sqrt{\mathbf{a}^T \mathbf{S}_a^{-1} \mathbf{a}}$ . The  $(S/N)^2$  is calculated over a grid of frequencies to produce an SIP. The  $(S/N)$  operation takes into account the goodness of fit, i.e. if the amplitude of the sinusoid at a given frequency is not well constrained, it is penalized.

### 3. Application to real light curves

An example LS periodogram of the raw *K2* photometry for giant star, EPIC 201183188 is shown in figure 1. Peaks appearing at  $47 \mu\text{Hz}$  and its harmonics are produced by the regular  $\sim 6$  hour thruster fires that repoint the spacecraft. These peaks are also present in periodograms of the VJ14 detrended light curves. The presence of systematic signals at these timescales are problematic for asteroseismic analysis since they lie in a region of frequency space that is often populated by giant asteroseismic modes. It is possible to remove these signals by ‘prewhitening’ the data, i.e. subtracting a sinusoid of that frequency from the data, however this process will artificially suppress all signals, both systematic and astrophysical, at that frequency. The SIP method eliminates the necessity for any such procedure. The bottom panel of figure 1 shows the SIP for the same star, demonstrating the ability of the SIP method to produce periodograms that are free from thruster firing signals.

In order to search for high signal-to-noise asteroseismic modes in the giant star candidates of GO1059, we searched for a power excess in the SIPs using the method of Huber et al. (2009): autocorrelation functions were calculated for sections of the SIP in order to search for regions of increased correlation and locate the frequency of maximum power. The increased correlation arises from the even frequency spacing of acoustic modes, and the frequency of maximum correlation at the location of the power excess corresponds to the large frequency separation,  $\Delta\nu$ . Figures 2(a) to 2(e) show example power spectra of 6 targets for which we detect pulsations using this method.

The top panel of figure 3 shows the VJ14-detrended light curve of an active, rotating star, EPIC 201133037, with a linear trend subtracted off. The brightness fluctuations clearly visible in the light curve of this target are produced by cool active regions on the stellar surface, which reduce the stellar flux periodically. The rotation period of this star is therefore around 20 days. The middle and bottom panels show an ACF and LS periodogram of the

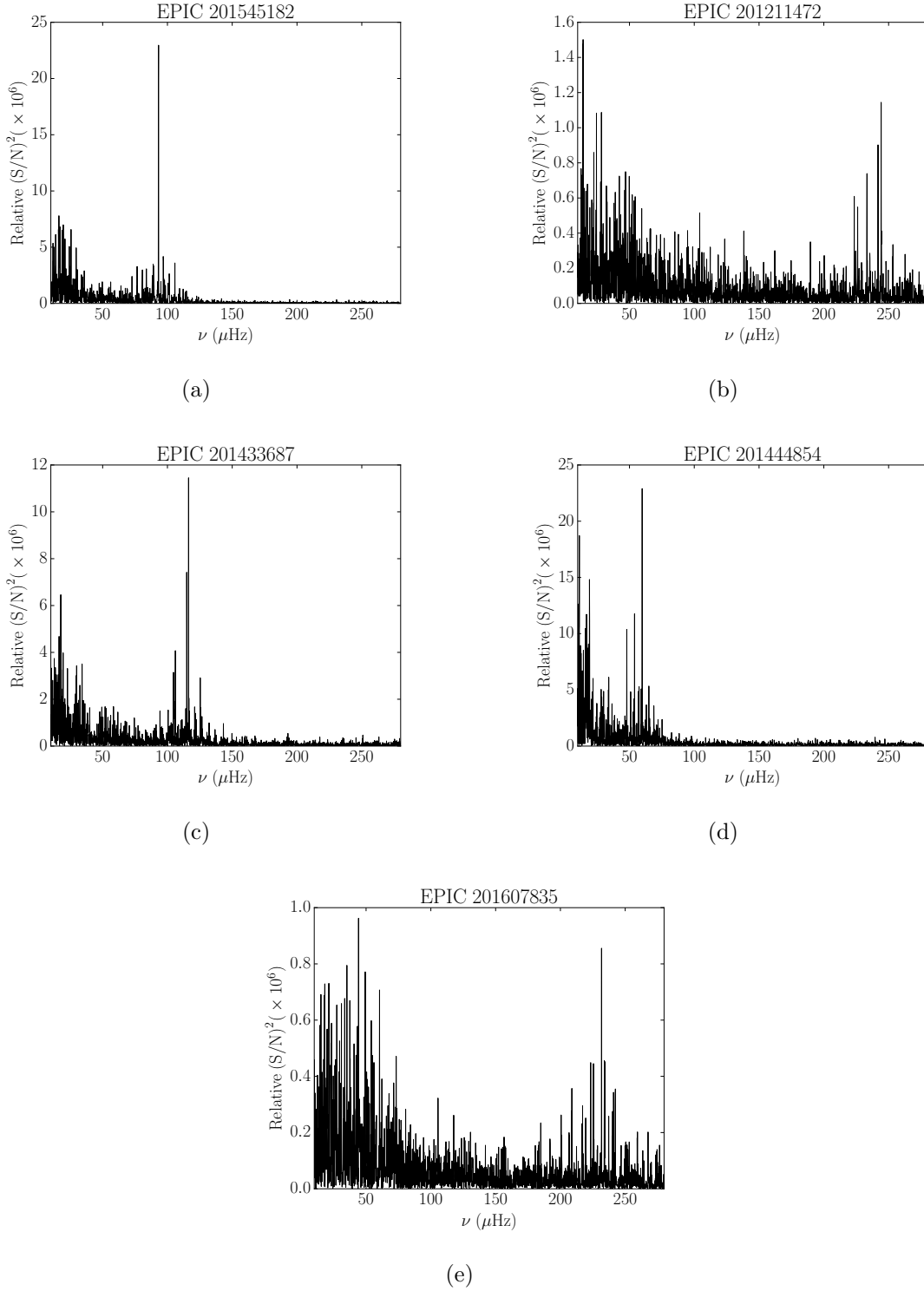


Fig. 2.— SIPs of 6 long cadence *K2* giants with asteroseismic oscillations. These were selected from the guest observing program, GO1059 and identified using the method of Huber et al. (2009).



detrended light curve. The top panel of figure 4 shows the raw light curve of the same target in grey, with the conditioned light curve in black. This conditioned light curve was produced by removing the best fitting systematic trends, described by a certain combination of the ELCs, at the best fitting period of the sinusoid. The bottom panel shows the SIP.

Each of these three methods measures a rotation period of around 20 days for this target. This example demonstrates the ability of the SIP to recover rotation periods that agree with those measured from detrended light curves by autocorrelation. We also include an example that demonstrates the ability of the SIP to outperform a periodogram of detrended data. Figure 5 shows the light curve, ACF and LS periodogram of another rotating star, EPIC 201142043 and figure 6 shows its SIP. This star shows lower amplitude variability than the previous example and the careful treatment of systematics is much more important. Whereas the ACF method is able to measure a rotation of  $\sim 3$  days for this star, the LS periodogram of the detrended light curve incorrectly measures a period of 59 days. Although there is a small peak at the rotation period of the star, it is not the dominant periodic signal. The SIP method is, by definition, insensitive to these long-term systematics and is able to measure a period of  $\sim 2$  days. This example further demonstrates the fact that long-term systematic trends caused by slow pointing variations are often not removed by conventional detrending methods. The 59 day signal is almost certainly a systematic trend and not an astrophysical signal because it does not appear in the SIP. It is well described by the ELCs and must therefore be common to many stars.

We have shown that the SIP method is able to measure stellar rotation periods and does better than producing periodograms from detrended data. However, it has been shown that the ACF method often performs better than periodogram methods in general for measuring stellar rotation periods (McQuillan et al. 2013a,b; Mazeh et al. 2015). For stars with relatively high-amplitude variability, for which perfect removal of systematic trends is less important, performing the ACF method on detrended data is likely to produce similar results to the SIP method. The SIP method is ideally suited to low-amplitude cases, where systematic trends could drastically influence rotation period measurements. Whilst the SIP method may outperform ACF in the low-amplitude cases, any ‘marginal’ rotation period measurements calculated using either method should be treated with caution unless a representative uncertainty is provided. In general neither ACF nor periodogram methods are equipped to provide such uncertainties. In practise, we recommend using both the SIP and ACF methods, in combination with a by-eye check, to measure rotation periods for *K2* stars.

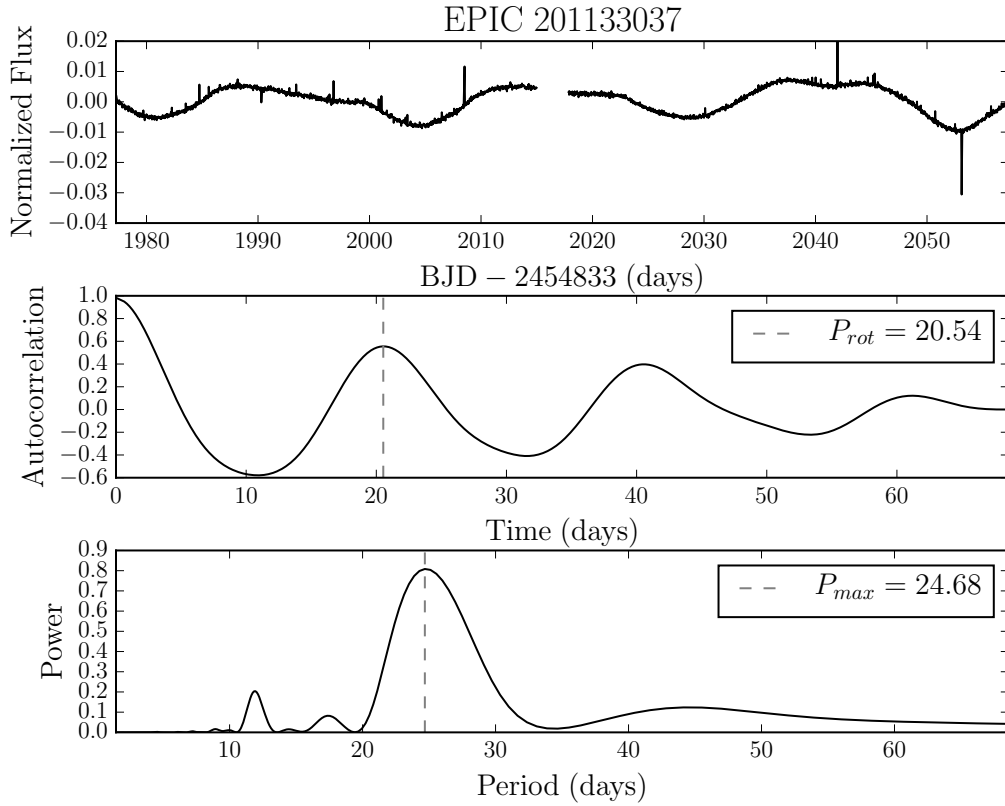


Fig. 3.— *Top*: Light curve of EPIC 201133037, detrended using the method of VJ14. *Middle*: Autocorrelation function of the detrended light curve. The autocorrelation function method measures a rotation period of 21 days for this star. *Bottom*: The LS periodogram of the detrended light curve. The highest peak in the periodogram is located at 25 days.

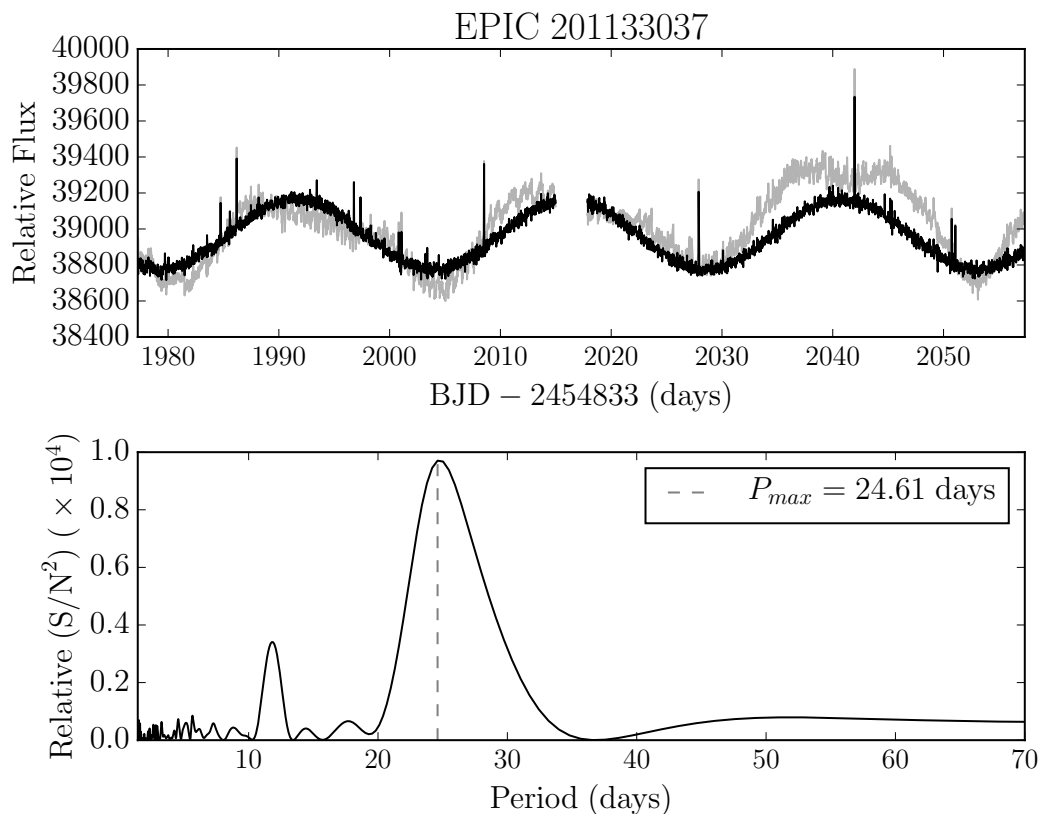


Fig. 4.— *Top*: The raw light curve of EPIC 201133037 is shown in grey and the conditioned light curve is shown in black. The conditioned light curve is produced by removing the trends that best describe the data, at the best fitting frequency. *Bottom*: An SIP of the raw light curve, produced by modelling the data using the top 150 ELCs plus a sine and cosine function at a range of frequencies. The highest peak in the SIP is located at 25 days.

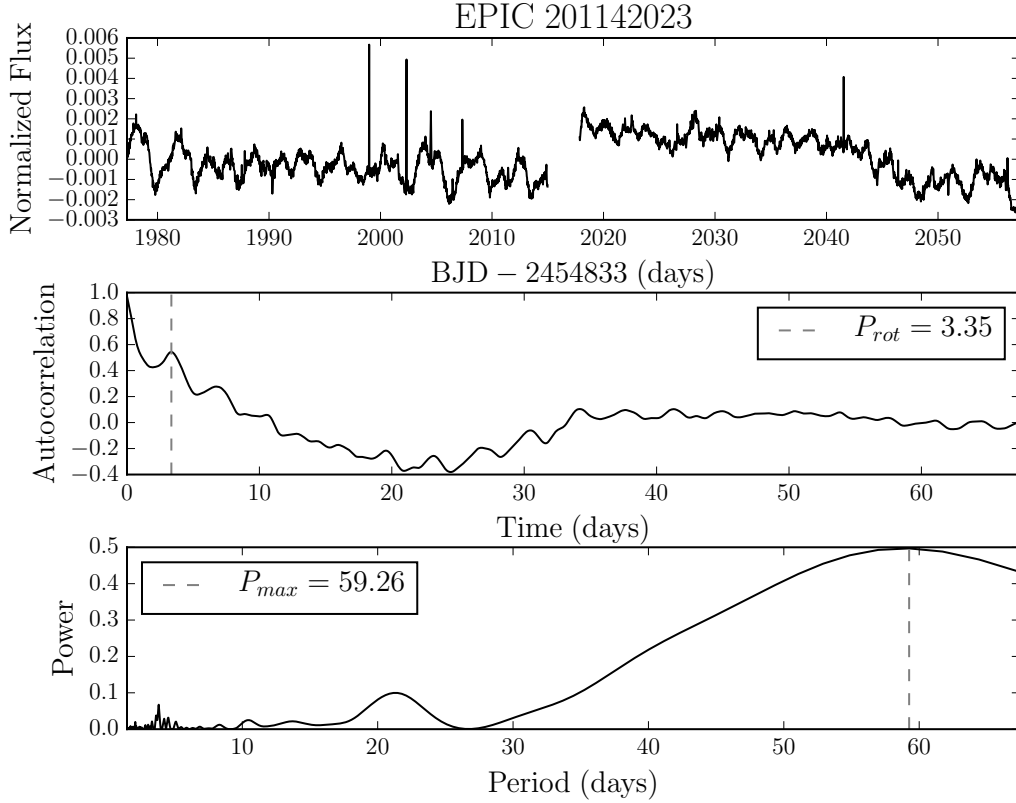


Fig. 5.— *Top*: Light curve of EPIC 201142043, detrended using the method of VJ14. *Middle*: Autocorrelation function of the detrended light curve. The autocorrelation function method measures a rotation period of 3 days for this star. *Bottom*: The LS periodogram of the detrended light curve. The highest peak in the periodogram is located at 59 days and is likely to be a systematic trend produced by spacecraft pointing variations.

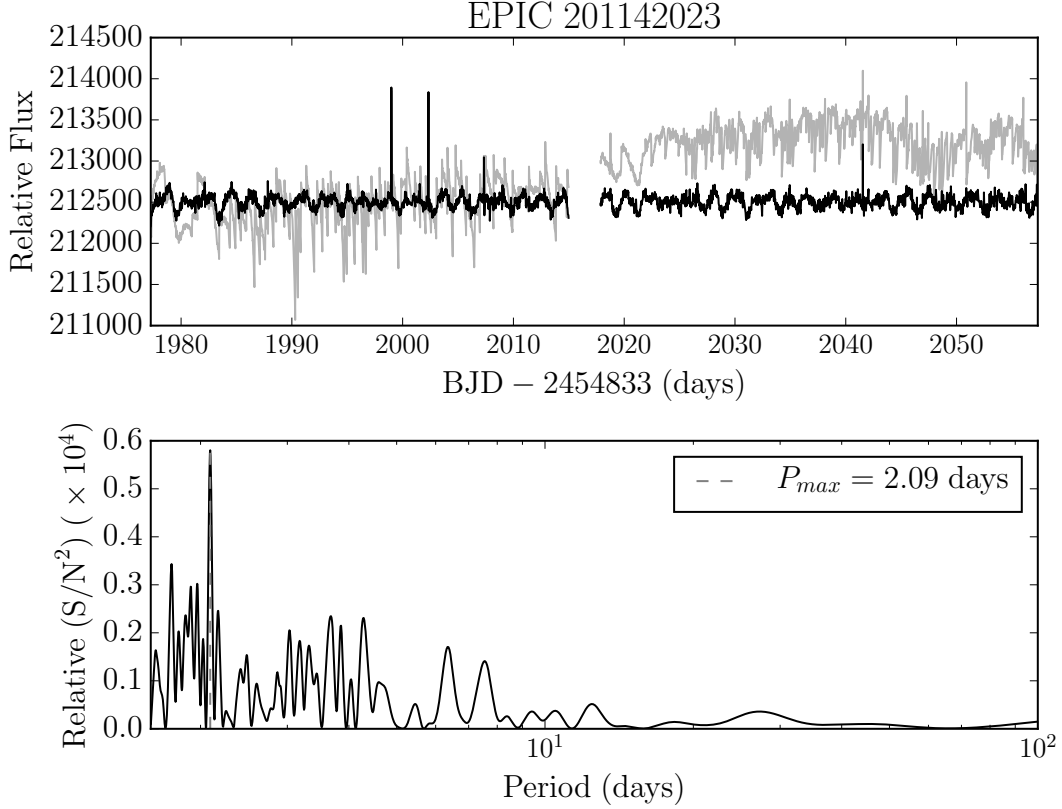


Fig. 6.— *Top*: The raw light curve of EPIC 201142043 is shown in grey and the conditioned light curve is shown in black. The conditioned light curve is produced by removing the trends that best describe the data, at the best fitting frequency. *Bottom*: An SIP, produced by modelling the data as a linear combination of the top 150 ELCs plus a sine and cosine function at a range of frequencies, measuring a rotation period of 2 days. The SIP is, by definition, insensitive to the long-timescale systematics that dominate the LS periodogram of the detrended data, shown in figure 5.

### 3.1. Tests and discussion

In order to demonstrate the consistent ability of the SIP method to remove the signal at  $47\mu\text{Hz}$ , corresponding to the periodic  $\sim 6$  hour thruster firings, we computed SIPs for 4923 targets from the GO1049 proposal: “Galactic Archaeology on a grand scale” (PI: Stello, D.). For each target, an SIP of its raw photometry and a LS periodogram of its VJ14 light curve was calculated for frequencies between 40 and  $54\mu\text{Hz}$ . Both the height and frequency of the highest peak in the SIP and the highest peak in the LS periodogram were recorded. A histogram of the frequencies of the highest peaks in the SIPs of all 4923 targets is shown in the top panel of figure 7. The bottom panel shows the histograms of peak heights within the correspondingly colored ranges indicated in the top panel. This figure shows that while there are a greater number of maximum peaks around  $47\mu\text{Hz}$ , the S/Ns of these peaks are comparable to those found just above and just below this frequency. Figure 8 shows the equivalent results for the VJ14 light curves. There is a significant number of large peaks at  $\sim 47\mu\text{Hz}$  in the LS periodograms of the detrended light curves; the highest peak in the LS periodograms was almost always located at  $\sim 47\mu\text{Hz}$ . Furthermore, the distribution of peak power within the range  $46.5\text{--}48\mu\text{Hz}$  is skewed towards higher powers, i.e. a substantial fraction of the peaks at  $\sim 47\mu\text{Hz}$  have a large power. The SIP method is able to consistently remove the  $47\mu\text{Hz}$  signal which is present in almost every VJ14 light curve.

Figures 9 and 10 show the conditioned light curves and SIPs of an RR Lyrae star, selected from Guest observer program GO1018; “Long Cadence RR Lyrae targets” (PI: Plachy, E.) and an Eclipsing Binary (EB), selected from the Armstrong et al. (2015) *K2* EB and variable star catalogue respectively. Figure 11 shows the conditioned light curve and SIP of the short-period, disintegrating planet candidate discovered by Sanchis-Ojeda et al. (2015). This planet has a period of around 9 hours, short enough to be detectable with a periodogram, as was demonstrated for a number of ultra-short period *Kepler* exoplanets by Sanchis-Ojeda et al. (2014). The top panels of these three figures show the *K2* light curves of these objects, conditioned on the highest S/N sinusoidal signal in the periodograms. These light curves were produced by subtracting the trends that best describe the data at the highest S/N period found in the SIP.

Photometric variability in dwarf stars on timescales less than 8 hours, often known as flicker, has been linked to surface gravity (Bastien et al. 2013; Kipping et al. 2014). The metrics used to quantify photometric variability include finding the range in intensity, counting the number of zero crossings and calculating the root-mean-square (RMS) of the light curve. Although these features are related to signal processing, they are operations performed on detrended light curves, not inferred from periodograms. However, it may be possible to derive a property of the periodogram that scales with the density or surface

gravity of a star, for example, the mean excess power at frequencies near those relevant to granulation timescales. The SIP method presented here would be useful for such a technique.

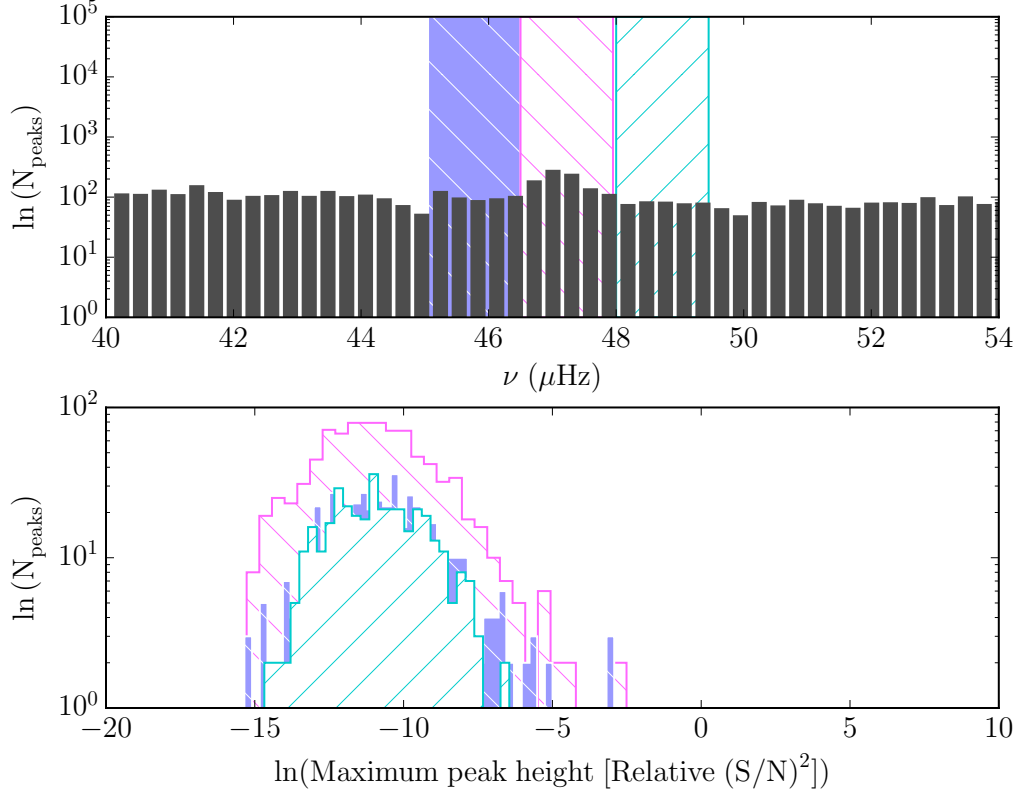


Fig. 7.— *Top*: Histogram of the frequencies of the highest peaks in the SIPs of 4923 *K2* targets within the range 40–54  $\mu\text{Hz}$ . *Bottom*: Histograms of peak heights within the correspondingly colored ranges indicated in the top panel. Whilst there is a larger number maximum peaks around 47  $\mu\text{Hz}$  (the frequency corresponding to the 6 hour thruster fire) the amplitudes of these maximum peaks are comparable to the maximum peak heights just above and just below this frequency.



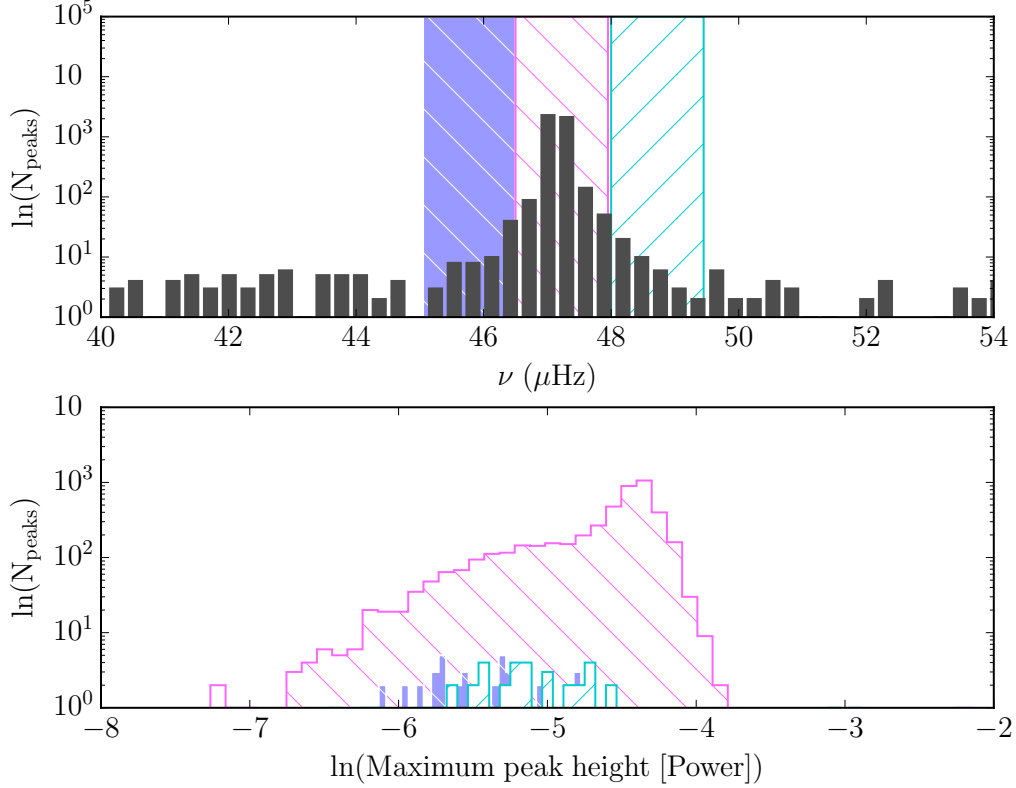


Fig. 8.— *Top*: Histogram of the frequencies of the highest peaks in the LS periodograms of the Vanderburg and Johnson (2014) light curves of 4923 *K2* targets within the range 40–54  $\mu\text{Hz}$ . *Bottom*: Histograms of peak heights within the correspondingly colored ranges indicated in the top panel. The frequency of maximum peak height was  $\sim 47 \mu\text{Hz}$  in almost every periodogram. Furthermore, the distribution of maximum peak height within the range 46.5–48  $\mu\text{Hz}$  is skewed towards higher powers, i.e. a large fraction of the peaks at  $\sim 47 \mu\text{Hz}$  have a large power.

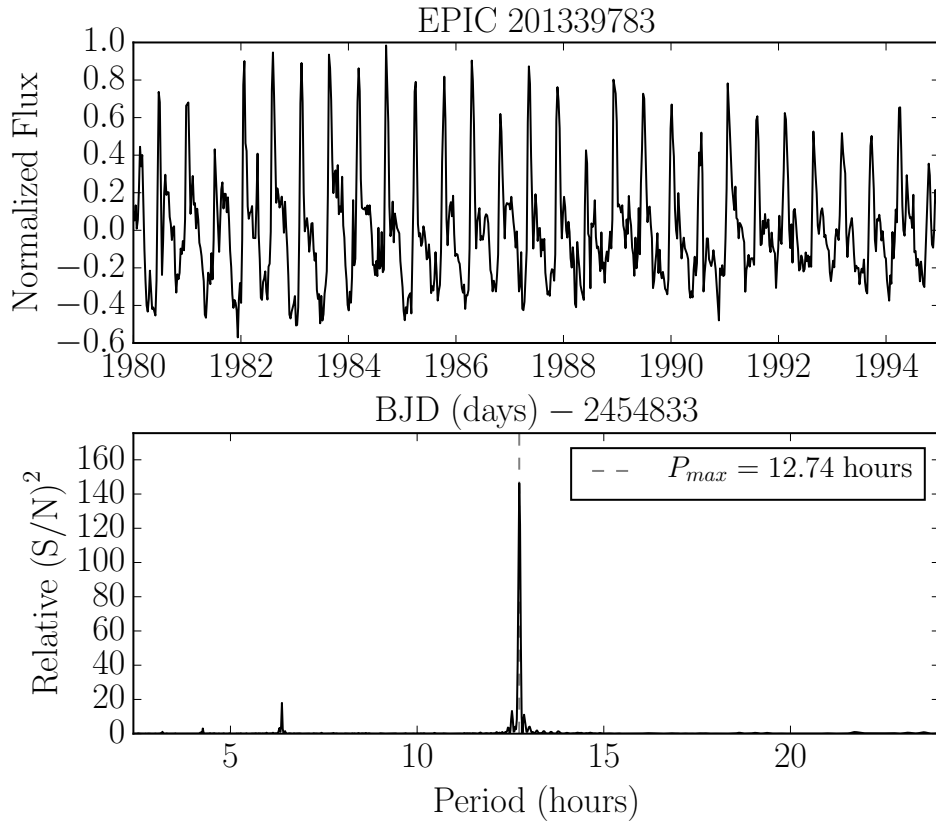


Fig. 9.— *Top*: The light curve of RR Lyrae star, EPIC 201339783, conditioned on the highest amplitude sinusoidal signal found in the SIP. *Bottom*: The systematic-insensitive periodogram of this light curve. This target was selected from GO1018 (PI: Plachy, E.).

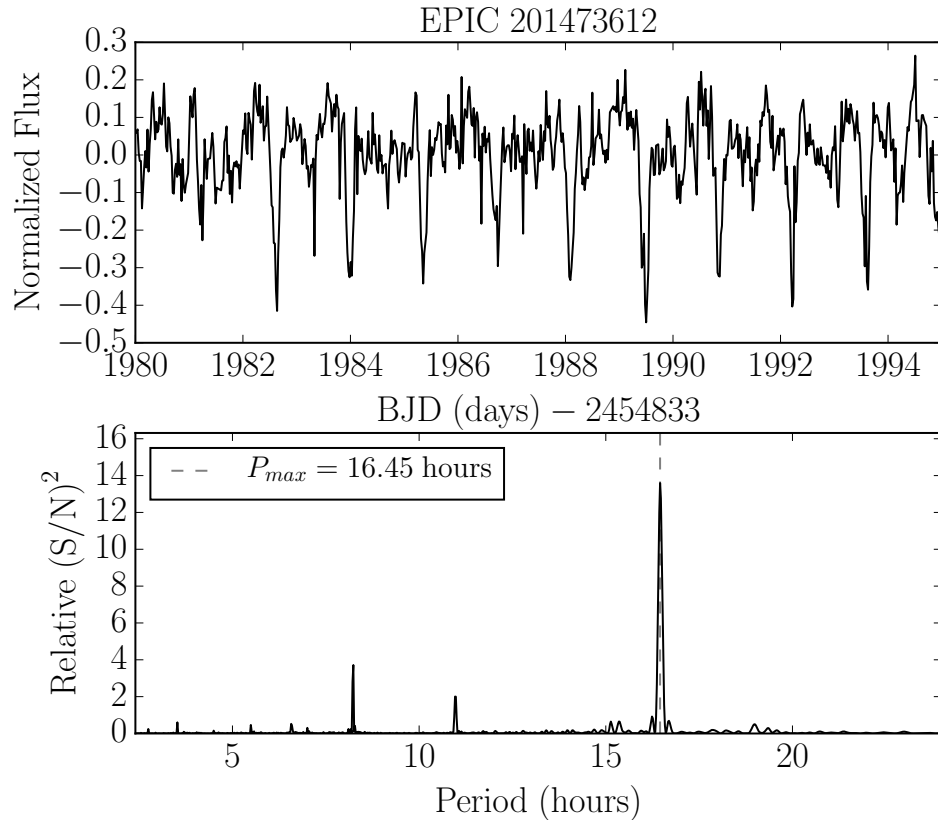


Fig. 10.— *Top*: The light curve of eclipsing binary, EPIC 201473612, conditioned on the highest amplitude sinusoidal signal found in the SIP. *Bottom*: The systematic-insensitive periodogram of this light curve. This target was selected from the catalogue of EBs and variable stars of Armstrong et al. (2015).

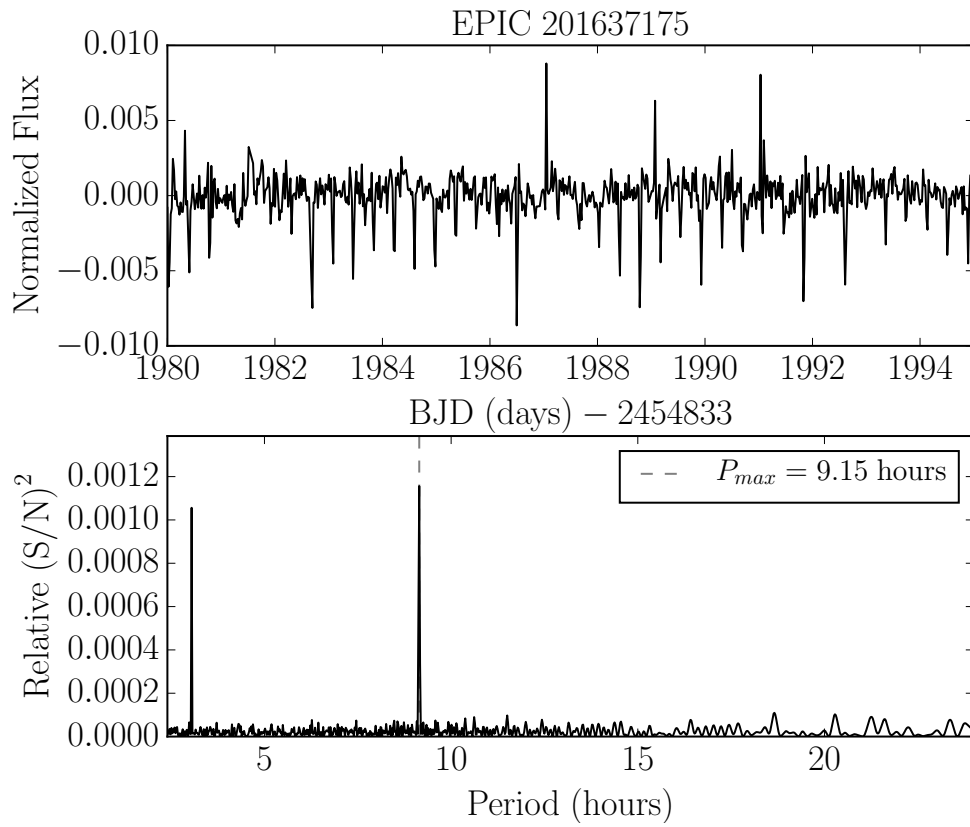


Fig. 11.— *Top*: The light curve of exoplanet candidate, EPIC 201637175, conditioned on the highest amplitude sinusoidal signal found in the periodogram. *Bottom*: The systematic-insensitive periodogram of this target.

## 4. Conclusions

We demonstrate that modelling campaign 1 *K2* photometry as a linear combination of 150 PCA components plus a sinusoid can produce periodograms that are almost completely free from instrumental systematic signals, without the need for detrending. We find that the 47  $\mu\text{Hz}$  signal, generated by the spacecraft thruster fires is not present in the vast majority of Systematics-Insensitive Periodograms (SIPs) for more than 4000 targets selected from the *K2* guest observer program, GO1059, “Galactic Archaeology on a grand scale” (PI: Stello, D.). The SIP method is highly successful for campaign 1 targets where the large number of stars, observed for a baseline of 80 days ensures that most of the systematics are captured in the ELCs and we anticipate that it will be equally effective for the up-and-coming campaigns.

The SIP method is capable of detecting periodicities in *K2* data in the region of frequency space relevant to the study of asteroseismic oscillations in giant stars and for any signals with a timescale close to 6 hours. It is also effective at measuring stellar rotation periods and is an improvement upon a simple LS periodogram of detrended data. In practise, the best approach for measuring rotation periods in *K2* data is likely to be a combination of the SIP method and the ACF method, where autocorrelation is performed on detrended light curves. The SIP code is available for public use and can be found at <https://github.com/RuthAngus/SIPK2>.

It is a pleasure to thank Dan Huber (Sydney) who provided many excellent comments for this paper and useful asteroseismology tips. We would also like to thank David Hogg (NYU) and Suzanne Aigrain (Oxford) for their comments, plus Andrew Vanderburg (Harvard), Ben Montet (Caltech) and Stephanie Douglas (Columbia) for their extremely helpful suggestions and recommendations regarding this project. J.A.J is supported by generous grants from the David and Lucile Packard and Alfred P. Sloan Foundations. The data presented in this paper were obtained from the Mikulski Archive for Space Telescopes (MAST). STScI is operated by the Association of Universities for Research in Astronomy, Inc., under NASA contract NAS5-26555. Support for MAST for non-HST data is provided by the NASA Office of Space Science via grant NNX09AF08G and by other grants and contracts. This paper includes data collected by the Kepler mission. Funding for the Kepler mission is provided by the NASA Science Mission directorate.

## REFERENCES

S. Aigrain, S. T. Hodgkin, M. J. Irwin, J. R. Lewis, and S. J. Roberts. Precise time series photometry for the Kepler-2.0 mission. *MNRAS*, 447:2880–2893, March 2015. doi:

10.1093/mnras/stu2638.

- R. Angus, S. Aigrain, D. Foreman-Mackey, and A. McQuillan. Calibrating gyrochronology using Kepler asteroseismic targets. *MNRAS*, 450:1787–1798, June 2015. doi: 10.1093/mnras/stv423.
- D. J. Armstrong, J. Kirk, K. W. F. Lam, et al. K2 Variable Catalogue II: Variable Stars and Eclipsing Binaries in K2 Fields 1 and 0. *ArXiv e-prints*, February 2015.
- S. A. Barnes. Ages for Illustrative Field Stars Using Gyrochronology: Viability, Limitations, and Errors. *ApJ*, 669:1167–1189, November 2007. doi: 10.1086/519295.
- F. A. Bastien, K. G. Stassun, G. Basri, and J. Pepper. An observational correlation between stellar brightness variations and surface gravity. *Nature*, 500:427–430, August 2013. doi: 10.1038/nature12419.
- B. Béky, M. J. Holman, D. M. Kipping, and R. W. Noyes. Stellar Rotation-Planetary Orbit Period Commensurability in the HAT-P-11 System. *ApJ*, 788:1, June 2014. doi: 10.1088/0004-637X/788/1/1.
- J. L. Christiansen, J. M. Jenkins, D. A. Caldwell, et al. The Derivation, Properties, and Value of Kepler’s Combined Differential Photometric Precision. *PASP*, 124:1279–1287, December 2012. doi: 10.1086/668847.
- I. J. M. Crossfield, E. Petigura, J. Schlieder, et al. A nearby M star with three transiting super-Earths discovered by K2. *ArXiv e-prints*, January 2015.
- C. R. Epstein and M. H. Pinsonneault. How Good a Clock is Rotation? The Stellar Rotation-Mass-Age Relationship for Old Field Stars. *ApJ*, 780:159, January 2014. doi: 10.1088/0004-637X/780/2/159.
- D. Foreman-Mackey, B. T. Montet, D. W. Hogg, et al. A systematic search for transiting planets in the K2 data. *ArXiv e-prints*, February 2015.
- R. A. García, S. Hekker, D. Stello, J. Gutiérrez-Soto, R. Handberg, D. Huber, C. Karoff, K. Uytterhoeven, T. Appourchaux, W. J. Chaplin, Y. Elsworth, S. Mathur, J. Ballot, J. Christensen-Dalsgaard, R. L. Gilliland, G. Houdek, J. M. Jenkins, H. Kjeldsen, S. McCauliff, T. Metcalfe, C. K. Middour, J. Molenda-Zakowicz, M. J. P. F. G. Monteiro, J. C. Smith, and M. J. Thompson. Preparation of Kepler light curves for asteroseismic analyses. *MNRAS*, 414:L6–L10, June 2011. doi: 10.1111/j.1745-3933.2011.01042.x.

- R. A. García, T. Ceillier, D. Salabert, et al. Rotation and magnetism of Kepler pulsating solar-like stars. Towards asteroseismically calibrated age-rotation relations. *A&A*, 572:A34, December 2014. doi: 10.1051/0004-6361/201423888.
- S. B. Howell, C. Sobeck, M. Haas, M. Still, T. Barclay, F. Mullally, J. Troeltzsch, S. Aigrain, S. T. Bryson, D. Caldwell, W. J. Chaplin, W. D. Cochran, D. Huber, G. W. Marcy, A. Miglio, J. R. Najita, M. Smith, J. D. Twicken, and J. J. Fortney. The K2 Mission: Characterization and Early Results. *PASP*, 126:398–408, April 2014. doi: 10.1086/676406.
- D. Huber, D. Stello, T. R. Bedding, et al. Automated extraction of oscillation parameters for Kepler observations of solar-type stars. *Communications in Asteroseismology*, 160: 74, October 2009.
- D. M. Kipping, F. A. Bastien, K. G. Stassun, et al. Flicker as a Tool for Characterizing Planets Through Asterodensity Profiling. *ApJ*, 785:L32, April 2014. doi: 10.1088/2041-8205/785/2/L32.
- M. N. Lund, R. Handberg, G. R. Davies, W. J. Chaplin, and C. D. Jones. K2P<sup>2</sup> A photometry pipeline for the K2 mission. *ArXiv e-prints*, April 2015.
- T. Mazeh, H. B. Perets, A. McQuillan, and E. S. Goldstein. Photometric Amplitude Distribution of Stellar Rotation of KOIs—Indication for Spin-Orbit Alignment of Cool Stars and High Obliquity for Hot Stars. *ApJ*, 801:3, March 2015. doi: 10.1088/0004-637X/801/1/3.
- A. McQuillan, S. Aigrain, and T. Mazeh. Measuring the rotation period distribution of field M dwarfs with Kepler. *MNRAS*, 432:1203–1216, June 2013a. doi: 10.1093/mnras/stt536.
- A. McQuillan, T. Mazeh, and S. Aigrain. Stellar Rotation Periods of the Kepler Objects of Interest: A Dearth of Close-in Planets around Fast Rotators. *ApJ*, 775:L11, September 2013b. doi: 10.1088/2041-8205/775/1/L11.
- K. Poppenhaefer and S. J. Wolk. Indications for an influence of hot Jupiters on the rotation and activity of their host stars. *A&A*, 565:L1, May 2014. doi: 10.1051/0004-6361/201423454.
- T. Reinhold and A. Reiners. Fast and reliable method for measuring stellar differential rotation from photometric data. *A&A*, 557:A11, September 2013. doi: 10.1051/0004-6361/201321161.

- R. Sanchis-Ojeda, S. Rappaport, J. N. Winn, et al. A Study of the Shortest-period Planets Found with Kepler. *ApJ*, 787:47, May 2014. doi: 10.1088/0004-637X/787/1/47.
- R. Sanchis-Ojeda, S. Rappaport, E. Pallé, et al. The K2-ESPRINT Project I: Discovery of the Disintegrating Rocky Planet with a Cometary Head and Tail EPIC 201637175b. *ArXiv e-prints*, April 2015.
- A. Skumanich. Time Scales for CA II Emission Decay, Rotational Braking, and Lithium Depletion. *ApJ*, 171:565, February 1972. doi: 10.1086/151310.
- J. C. Smith, M. C. Stumpe, J. E. Van Cleve, et al. Kepler Presearch Data Conditioning II - A Bayesian Approach to Systematic Error Correction. *PASP*, 124:1000–1014, September 2012. doi: 10.1086/667697.
- M. C. Stumpe, J. C. Smith, J. E. Van Cleve, et al. Kepler Presearch Data Conditioning I - Architecture and Algorithms for Error Correction in Kepler Light Curves. *PASP*, 124:985–999, September 2012. doi: 10.1086/667698.
- A. Vanderburg and J. A. Johnson. A Technique for Extracting Highly Precise Photometry for the Two-Wheeled Kepler Mission. *PASP*, 126:948–958, December 2014. doi: 10.1086/678764.
- A. Vanderburg, B. T. Montet, J. A. Johnson, et al. Characterizing K2 Planet Discoveries: A Super-Earth Transiting the Bright K Dwarf HIP116454. *ApJ*, 800:59, February 2015. doi: 10.1088/0004-637X/800/1/59.